A Low-Complexity I/Q Imbalance Calibration Method for Quadrature Modulator

Jusung Kim, Han-Shin Jo, Kyoung-Jae Lee, Dong-Ho Lee, Dae-Hyun Choi, and Sangkil Kim

*Abstract***—This brief presents a low-complexity I/Q (in-phase and quadrature components) imbalance calibration method for the transmitter using quadrature modulation. Impairments in analog quadrature modulator have a deleterious effect on the signal fidelity. Among the critical impairments, I/Q imbalance (gain and phase mismatches) deteriorates the residual sideband performance of the analog quadrature modulator degrading the error vector magnitude. Based on the theoretical mismatch analysis of the quadrature modulator, we propose a low-complexity I/Q imbalance extraction algorithm. After the parameter extraction, the transmitter is calibrated by imposing the counter imbalanced mismatch of the transmitter through the digital baseband. In comparison with existing I/Q imbalance calibration methods, the novelty of the proposed method lies in that: 1) only three spectrum measurements of the device-under-test are needed for extraction and calibration of gain and phase mismatches; 2) due to the blind nature of the calibration algorithm, the proposed approach can be readily applicable to an existing I/Q transmitter; 3) no extra hardware that degrades the calibration accuracy is required; and 4) due to the noniterative nature, the proposed method is faster and computationally more efficient than previously published methods.**

*Index Terms***—Calibration, image rejection, quadrature mismatch, quadrature modulation, residual sideband (RSB), single sideband, transmitter.**

I. Introduction

Analog quadrature modulator (direct conversion transmitter) offers compact and low-cost implementation. The simplicity of the topology makes it attractive for high level of integration. However, imperfections from gain and phase mismatches as well as dc offset deteriorate the out-of-band emission performance. Therefore, it requires the compensation for these errors, either with a digital signal processor (DSP) or analog circuits [1].

Many works based on the DSP techniques were proposed to compensate for I/Q imbalance. Sen *et al.* [2] utilized equation-based optimum test stimulus and power detection based on nonlinear phase-to-amplitude conversion. Witt and van Rooyen [3] presented an I/Q imbalance extraction algorithm utilizing the Cholesky decomposition of the signal's covariance matrix. Valkama *et al.* [4] proposed special reference signal generation to adaptively compensate for I/Q imbalance. However, DSP-based compensation is computationally intensive so that it requires extensive resources. Furthermore, extraction of mismatch parameters relies on nonlinear estimation, and thus convergence is not guaranteed.

Manuscript received June 25, 2018; revised September 11, 2018 and October 25, 2018; accepted November 24, 2018. This work was supported by Korea Government (MSIP) through the Institute for Information and Communications Technology Promotions (IITP) under Grant 2017-0-00659. *(Corresponding author: Sangkil Kim.)*

J. Kim, H.-S. Jo, and K.-J. Lee are with the Department of Electronics and Controls Engineering, Hanbat National University, Daejeon 34158, South Korea.

D.-H. Lee is with the Department of Information and Communication Engineering, Hanbat National University, Daejeon 34158, South Korea.

D.-H. Choi is with the School of Electrical and Electronics Engineering, Chung-Ang University, Seoul 156-756, South Korea.

S. Kim is with the Department of Electronics Engineering, Pusan National University, Pusan 46241, South Korea (e-mail: ksangkil3@pusan.ac.kr).

Color versions of one or more of the figures in this paper are available online at http://ieeexplore.ieee.org.

Digital Object Identifier 10.1109/TVLSI.2018.2883758

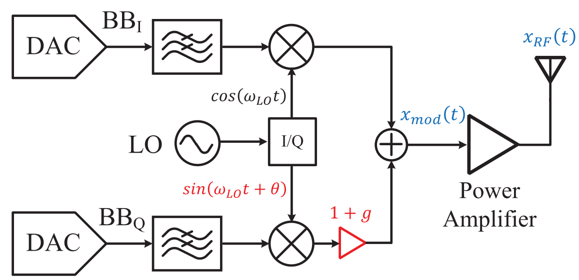

Fig. 1. Quadrature modulation-based transmitter architecture.

Analog techniques for I/Q imbalance compensation can be done with either loop-back receiver measurement [5]–[7] or baseband signal tuning based on the spectrum measurement [8], [9]. In [6], in-phase and quadrature baseband signals are transmitted sequentially and this time-sequenced injection method enables the calculation of quadrature mismatch parameters by measuring quadrature loop-back receiver outputs. Similarly, the work in [7] utilized two consecutive measurements with different attenuation settings. However, extraction of transmitter I/Q imbalance with the loop-back method is disturbed by the limited residual sideband (RSB) performance of the receiver. Coupling between the loop-back receiver and the transmitter further degrades the accuracy of the loop-back method.

In [8], local-oscillator (LO) feedthrough is first canceled by compensating signal due to on-chip digital to analog converter (DAC). I/Q imbalance is then compensated manually by adjusting the gain and phase of quadrature baseband signals. Patent from [9] depicts the same idea of adjusting the gain and phase of the quadrature baseband signals. Note that the works in [5]–[7] compute (extract) the gain and phase imbalance parameters with specially designed input sequence and the loop-back receiver. On the other hand, [8] and [9] cannot compute the imbalance parameters but manually adjust the baseband signals to improve the RSB performance based on the spectrum measurement.

In this brief, we propose a low-complexity I/Q imbalance extraction and calibration algorithm for an analog quadrature modulator. The algorithm requires three spectrum measurements with different test stimulus. The proposed method is noniterative and computes the I/Q imbalance parameters unambiguously. No extra hardware such as a loop-back receiver is required, consequently leading to accurate parameter extraction of the device-under-test (DUT).

II. Proposed I/Q Imbalance Calibration Method

In general, all the analog components such as filter, up-conversion mixer, and DAC of the I/Q branches contribute to the imbalance. Sources of all the gain mismatches can be aggregated into a single parameter g. Similarly, a parameter θ denotes the amalgamated phase mismatch of the transmitter. Then, a generalized block diagram of a direct-conversion transmitter is presented in Fig. 1. Up-converting

This article has been accepted for inclusion in a future issue of this journal. Content is final as presented, with the exception of pagination.

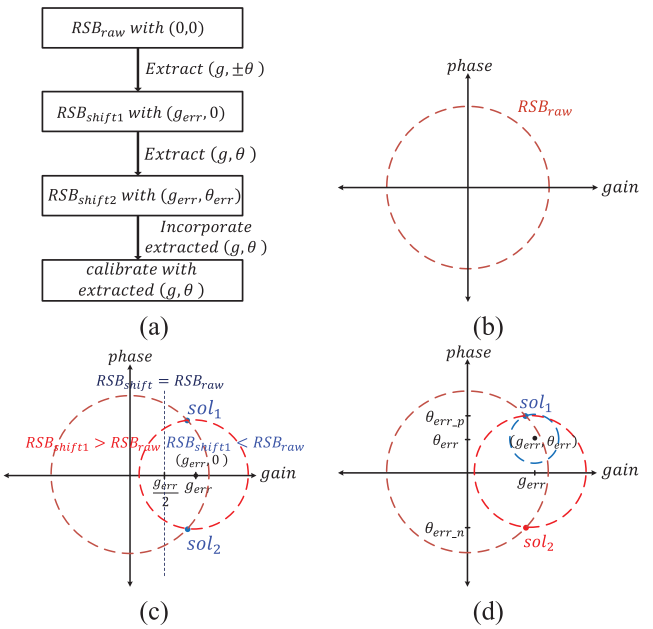

Fig. 2. Proposed extraction method and its procedure. (a) Flowchart of I/Q imbalance calibration. (b) Raw RSB. (c) RSB with gain mismatch (g_{err}). (d) RSB with gain and phase mismatch (g_{err}, θ_{err}).

signal $x_{\mathrm{LO}}(t)$ due to the quadrature modulator is expressed as

$$\begin{aligned} x_{\mathrm{LO}}(t) &= \cos(\omega_{\mathrm{LO}}t) + j(1+g)\sin(\omega_{\mathrm{LO}}t+\theta) \\ &= K_1 e^{j\omega_{\mathrm{LO}}t} + K_2 e^{-j\omega_{\mathrm{LO}}t} \end{aligned} \tag{1}$$

where the imbalance coefficients K_1 and K_2 are given by

$$K_1 = \frac{1}{2}(1+(1+g)e^{j\theta}) \tag{2}$$

$$K_2 = \frac{1}{2}(1-(1+g)e^{-j\theta}). \tag{3}$$

With positive baseband signal ($x_{\mathrm{BB}}(t) = e^{j\omega_{\mathrm{BB}}t}$), the transmitter output signal ($x_{\mathrm{RF}}(t)$) is written by

$$\begin{aligned} x_{\mathrm{RF}}(t) &= \mathbf{Re}[x_{\mathrm{BB}}(t)\cdot x_{\mathrm{LO}}(t)] \\ &= \mathbf{Re}[K_1]\cos(\omega_{\mathrm{usb}}t) - \mathbf{Im}[K_1]\sin(\omega_{\mathrm{usb}}t) \\ &\quad + \mathbf{Re}[K_2]\cos(\omega_{\mathrm{lsb}}t) + \mathbf{Im}[K_2]\sin(\omega_{\mathrm{lsb}}t) \end{aligned} \tag{4}$$

where $\omega_{\mathrm{usb}} = \omega_{\mathrm{LO}} + \omega_{\mathrm{BB}}$ and $\omega_{\mathrm{lsb}} = \omega_{\mathrm{LO}} - \omega_{\mathrm{BB}}$ denote the transmitted signal located at the upper sideband and lower sideband frequencies with respect to ω_{LO}. With no mismatches ($g = 0$ and $\theta = 0$) between I/Q branches, K_1 and K_2 are set to 1 and 0, respectively. Then, the transmitted signal has only the single tone at the upper sideband frequency of ω_{LO} as desired. The power ratio between upper sideband and lower sideband signal is RSB suppression ratio whose expression is

$$\begin{aligned} \mathrm{RSB_{raw}} &= \frac{(\mathrm{Power})_{\mathrm{lsb}}}{(\mathrm{Power})_{\mathrm{usb}}} = \frac{\mathbf{Re}^2[K_2]+\mathbf{Im}^2[K_2]}{\mathbf{Re}^2[K_1]+\mathbf{Im}^2[K_1]} = \frac{|K_2|^2}{|K_1|^2} \\ &= \frac{1-2(1+g)\cos(\theta)+(1+g)^2}{1+2(1+g)\cos(\theta)+(1+g)^2}. \end{aligned} \tag{5}$$

Under small imbalance conditions (e.g., $g < 0.1$, $\theta < 3°$), $\mathrm{RSB_{raw}}$ can be approximated as

$$\mathrm{RSB_{raw}} \approx \frac{(g)^2+(\theta)^2}{4}. \tag{6}$$

The derivation mentioned earlier includes the implicit assumption that there is no I/Q mismatch due to the baseband signal. The assumption is valid since the digital baseband can generate very accurate

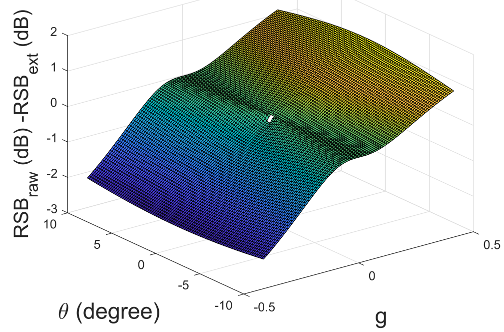

Fig. 3. Extraction accuracy of the proposed algorithm with the gain imbalance ($g \in \{-(\sqrt{2}-1), +(\sqrt{2}-1)\}$) and phase imbalance ($\theta \in \{-10°, +10°\}$).

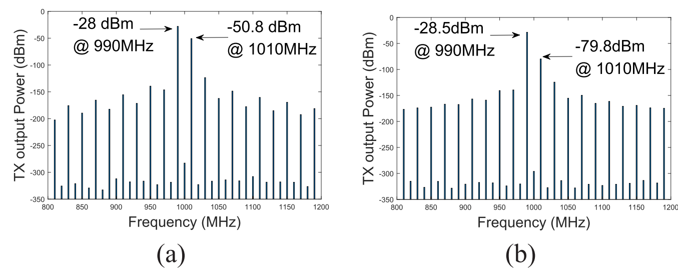

Fig. 4. Transmitter output spectrum with 10-MHz baseband and 1-GHz LO signals under $g = 0.122$ (1-dB imbalance) and $\theta = 5°$ conditions. (a) Before calibration. (b) After calibration.

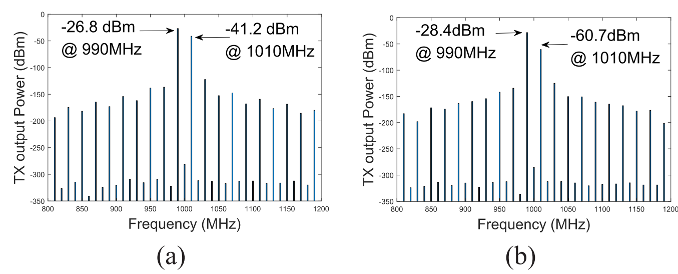

Fig. 5. Transmitter output spectrum with 10-MHz baseband and 1-GHz LO signals under $g = \sqrt{2}-1$ (3-dB imbalance) and $\theta = 10°$ conditions. (a) Before calibration. (b) After calibration.

quadrature signal in contrary to analog quadrature transmitter. Note that the power amplifier does not create any quadrature mismatch and its transfer function can be assumed to be unity here, i.e., $x_{\mathrm{RF}}(t) = x_{\mathrm{mod}}(t)$. With the mismatch parameters at the baseband ($-g_{\mathrm{err}}$ and θ_{err} for gain and phase mismatches, respectively), the baseband signal is evaluated in the following. Negative sign of the gain mismatch parameter ($-g_{\mathrm{err}}$) is introduced for computational convenience

$$\begin{aligned} x_{\mathrm{BB}}(t) &= \cos(\omega_{\mathrm{BB}}t) + j(1-g_{\mathrm{err}})\sin(\omega_{\mathrm{BB}}t+\theta_{\mathrm{err}}) \\ &= J_1 e^{j\omega_{\mathrm{BB}}t} + J_2 e^{-j\omega_{\mathrm{BB}}t} \end{aligned} \tag{7}$$

where the baseband imbalance coefficients J_1 and J_2 are given by

$$J_1 = \frac{1}{2}(1+(1-g_{\mathrm{err}})e^{j\theta_{\mathrm{err}}}) \tag{8}$$

$$J_2 = \frac{1}{2}(1-(1-g_{\mathrm{err}})e^{-j\theta_{\mathrm{err}}}). \tag{9}$$

TABLE I
COMPARISON OF THE PROPOSED ALGORITHM WITH PUBLISHED RESULTS

	RSB_{raw} (dB)	RSB_{cal} (dB)	Δ (dB)	Test Condition	Architecture
[8]	-34	-49.6	15.6	$f_{LO} = 5.24$GHz $f_{BB} = 1$MHz	Off-chip spectrum measurement and calibration without parameter extraction
[11]	-34.7	-56.1	21.4	$f_{LO} = 1$GHz $f_{BB} = 5$MHz	Off-chip spectrum measurement and calibration with parameter extraction
[12]	-38.5	-52.2	13.7	$f_{LO} = 1$GHz $f_{BB} = 5$MHz	Off-chip spectrum measurement and calibration with parameter extraction
[13]	-26	-56	30	$f_{LO} = 1.6$GHz $f_{BB} = 10$MHz	On-chip self-correction
This work	**-22.8**	**-51.3**	**28.5**	$f_{LO} = 1$GHz $f_{BB} = 10$MHz	**Off-chip spectrum measurement and calibration with parameter extraction**

With imbalanced baseband signal ($x_{\mathrm{BB}}(t)$) and up-converting signal ($x_{\mathrm{LO}}(t)$), the transmitter output signal ($x_{\mathrm{RF}}(t)$) can be derived as

$$\begin{aligned} x_{\mathrm{RF}}(t) = &\ \mathbf{Re}[J_1K_1 + J_2K_2]\cos(\omega_{\mathrm{usb}}t) \\ &+ \mathbf{Im}[-J_1K_1 + J_2K_2]\sin(\omega_{\mathrm{usb}}t) \\ &+ \mathbf{Re}[J_1K_2 + J_2K_1]\cos(\omega_{\mathrm{lsb}}t) \\ &+ \mathbf{Im}[J_1K_2 - J_2K_1]\sin(\omega_{\mathrm{lsb}}t). \end{aligned} \tag{10}$$

Following the same procedure with the ideal baseband signal case (4) and (5), RSB for transmitter output ($x_{\mathrm{RF}}(t)$) including the mismatches at both baseband signal and up-converting signal can be written as

$$\mathrm{RSB} = \frac{1 - 2(1+g)(1-g_{\mathrm{err}})\cos(\theta - \theta_{\mathrm{err}}) + [(1+g)(1-g_{\mathrm{err}})]^2}{1 + 2(1+g)(1-g_{\mathrm{err}})\cos(\theta + \theta_{\mathrm{err}}) + [(1+g)(1-g_{\mathrm{err}})]^2}. \tag{11}$$

With small imbalance conditions for both baseband and up-converting signal I/Q branch, RSB is approximated as

$$\mathrm{RSB} \approx \frac{(g - g_{\mathrm{err}})^2 + (\theta - \theta_{\mathrm{err}})^2}{4}. \tag{12}$$

Equations (6) and (12) indicate that RSB in (g,θ) plane is represented as a circle with radius ($2\sqrt{\mathrm{RSB}}$) centered at (g_{err}, θ_{err}). With the aim of obtaining gain and phase mismatch parameters (g, θ) in the form of a circle, three measurements are necessary to be performed. While many permutations of test stimulus exists, Fig. 2 shows the mismatch parameter extraction and its calibration method [Fig. 2(a)], and the mismatch parameter extraction procedure [Fig. 2(b)–(d)] without loss of generality.

The first measurement with no baseband mismatch condition [Fig. 2(b)] dictates that any gain and phase mismatches of the transmitter on the same radius can be a possible solution. The second measurement with baseband gain mismatch introduced [Fig. 2(c)] gives the definite solution for the gain mismatch but an indefinite solution for the phase mismatch parameter, whose solutions are derived as follows:

$$g = \frac{g_{\mathrm{err}}}{2} + \frac{2}{g_{\mathrm{err}}}(\mathrm{RSB_{raw}} - \mathrm{RSB_{shift1}}) \tag{13}$$

$$\theta = \pm\sqrt{4\mathrm{RSB_{raw}} - g^2}. \tag{14}$$

$\mathrm{RSB_{raw}} = \mathrm{RSB_{shift1}}$ dictates that the gain mismatch solution is $g = (g_{\mathrm{err}}/2)$. Otherwise, $\mathrm{RSB_{raw}} \gtrless \mathrm{RSB_{shift1}}$ gives $g \gtrless (g_{\mathrm{err}}/2)$. Finally, using the third measurement with both gain and phase imbalances of the baseband [Fig. 2(d)], the indefinite solution for the phase mismatch is determined without ambiguity. $\mathrm{RSB_{shift2}} \gtrless \mathrm{RSB_{shift1}}$ dictates that the phase mismatch is $\theta = \mp(4\mathrm{RSB_{raw}} - g^2)^{1/2}$ (sol_2 and sol_1 in Fig. 2).

III. SIMULATION RESULTS

The simulation results verify the validity of the proposed I/Q mismatch extraction and its calibration method. Fig. 3 shows the RSB difference due to the transmitter I/Q mismatch and the extracted RSB with the proposed method. Impairment due to the transmitter I/Q gain imbalance varies $g \in \{-(\sqrt{2}-1), +(\sqrt{2}-1)\}$ corresponding to the gain imbalance of ± 3 dB. The phase mismatch is introduced for $\theta \in \{-10^\circ, +10^\circ\}$. The simulation result shows that the extracted RSB ($\mathrm{RSB_{ext}}$) tracks the raw RSB ($\mathrm{RSB_{raw}}$) (< -14.3 dB when $g = \sqrt{2}-1$ and $\theta = 10^\circ$) with < 2.3 dB difference [$\mathrm{RSB_{raw}}$ (dB) $-$ $\mathrm{RSB_{ext}}$ (dB)].

Figs. 4 and 5 demonstrate the Spectre simulation results for the proposed calibration method. The voltage mode passive mixer similar to [10] was designed in double-balanced configuration. Then, the imbalance was imposed on the LO signals with an ideal voltage source. Then, extracted g_{err} and θ_{err} with the proposed extraction method were injected from the baseband with counter-imbalanced fashion. We adopted the voltage mode passive mixer for the verification since there is no additional transfer function between the mismatched sources and DUT, which distorts the verification results. The frequencies of the baseband signal and LO signals were set at $\omega_{\mathrm{BB}} = 10$ MHz and $\omega_{\mathrm{LO}} = 1$ GHz.

Fig. 4 depicts the simulation results with modest imbalances at $g = 0.122$ (1-dB imbalance) and $\theta = 5^\circ$. The proposed calibration method improves the RSB from -22.8 to -51.3 dB with 28.5-dB improvement. The simulation result with significant imbalances at $g = \sqrt{2} - 1$ (3-dB imbalance) and $\theta = 10^\circ$ is shown in Fig. 5. The improvement due to the proposed algorithm reaches 18 dB. Although the approximations in (6) and (12) require small imbalance conditions such as $g < 0.1$, $\theta < 3^\circ$, the simulation results demonstrate that the calibration works well for larger gain and phase imbalances.

The calibration performance compared to the reported research efforts is depicted in Table I. The work in [13] enables the online calibration for the Weaver image-reject receiver architecture. For the calibration of the receiver I/Q mismatch, the online calibration is relatively easier since both in-phase and quadrature-phase signals at baseband frequency are accessible separately on chip. The work in [8] employs the predistortion method after measuring the transmitter output spectrum off-chip without extracting DUT's gain and phase imbalance parameters. In [11], [12], calibration is performed after extracting the quadrature mismatch parameters. The extraction algorithm is complex and the quadrature mismatch parameters are distorted by the additional diode employed in their works. Compared to previous works [8], [11], [12], our extraction method is

TABLE II
PERFORMANCE SUMMARY OF THE PROPOSED ALGORITHM

Imbalance Condition	g	g_{err}	θ_{err}	RSB_{raw} (dB)	RSB_{cal} (dB)	Δ (dB)
1dB & 3°	0.122	0.115	2.92	-24	-49.9	25.9
1dB & 5°	0.122	0.115	4.95	-22.8	-51.3	28.5
2dB & 5°	0.259	0.234	4.04	-18.2	-37.9	19.7
2dB & 7°	0.259	0.234	7.45	-17.7	-39.6	21.9
3dB & 10°	0.412	0.35	9.15	-14.3	-32.3	18

computationally more efficient and requires less number of spectrum measurements. Under more severe imbalance condition ($\mathrm{RSB_{raw}}$), the proposed work calibrates the RSB performance to the similar level (e.g., RSB < -50 dB).

Performance summary of the extraction algorithm and its calibrated result is shown in Table II. Extraction accuracy of the proposed algorithm outperforms previous works based on the loop-back receiver measurement. For instance, the work in [6] reports $\theta_{\mathrm{err}} = 1.58°$ and $5.43°$ for phase imbalance of $1°$ and $3°$, respectively.

IV. CONCLUSION

In this brief, low-complexity I/Q Imbalance extraction and its calibration method are proposed to counter-imbalance the finite RSB of the direct conversion transmitter. The structure of an analog quadrature modulator I/Q imbalance is analyzed, and it is proven that the RSB in (g, θ) plane is expressed using the Cartesian representation of a circle centered at $(g_{\mathrm{err}}, \theta_{\mathrm{err}})$.

The proposed approach is conducted in a noniterative manner using only three measurements to calculate the imbalance parameters of the analog quadrature modulator. The calibration is performed by incorporating the counter imbalanced mismatch parameters through the digital baseband offering high accuracy. The simulation results verify that the proposed method can extract the RSB with < 2.3 dB accuracy under the imbalance condition ($|g| < \sqrt{2} - 1$, $|\theta| < 10°$). The RSB improvement due to the proposed method is verified with the specter simulation test bench.

The proposed calibration method is only applicable to offline calibration and thus it does not calibrate the dynamic environmental changes such as temperature drift and aging. The extraction requires high-precision spectrum analyzer. However, our proposed method allows faster extraction time and swift calibration without any ambiguity. The reduction in calibration time corresponds to the reduced cost for testing. Extraction and calibration performances do not have to be sacrificed with our approach since no additional circuits are required in DUT nor external environment.

REFERENCES

[1] J. K. Cavers, "New methods for adaptation of quadrature modulators and demodulators in amplifier linearization circuits," *IEEE Trans. Veh. Technol.*, vol. 46, no. 3, pp. 707–716, Aug. 1997.

[2] S. Sen, S. K. Devarakond, and A. Chatterjee, "DSP assisted low cost IQ mismatch measurement and compensation using built in power detector," in *IEEE MTT-S Int. Microw. Symp. Dig.*, May 2010, pp. 336–339.

[3] J. J. de Witt and G.-J. Van Rooyen, "A blind I/Q imbalance compensation technique for direct-conversion digital radio transceivers," *IEEE Trans. Veh. Technol.*, vol. 58, no. 4, pp. 2077–2082, May 2009.

[4] M. Valkama, M. Renfors, and V. Koivunen, "Advanced methods for I/Q imbalance compensation in communication receivers," *IEEE Trans. Signal Process.*, vol. 49, no. 10, pp. 2335–2344, Oct. 2001.

[5] L. K. Leung, C. Narathong, and J. Hu, "Transmitter residual sideband and local oscillator leakage calibration using a reconfigurable tone generator and lo paths," U.S. Patent 20 150 118 980 A1, Apr. 30, 2015.

[6] A. Nassery and S. Ozev, "An analytical technique for characterization of transceiver IQ imbalances in the loop-back mode," in *Proc. Design, Autom. Test Eur. Conf. Exhibit.*, Mar. 2012, pp. 1084–1089.

[7] E. S. Erdogan and S. Ozev, "Detailed characterization of transceiver parameters through loop-back-based BiST," *IEEE Trans. Very Large Scale Integr. (VLSI) Syst.*, vol. 18, no. 6, pp. 901–911, Jun. 2010.

[8] C. P. Lee *et al.*, "A highly linear direct-conversion transmit mixer transconductance stage with local oscillation feedthrough and I/Q imbalance cancellation scheme," in *IEEE Int. Solid State Circuits Conf. (ISSCC) Dig. Tech. Papers*, Feb. 2006, pp. 1450–1459.

[9] M. Dale and W. H. Thesling, "Residual carrier and side band processing system and method," U.S. Patent 7 443 924 B2, Oct. 28, 2008.

[10] H. Khatri, P. S. Gudem, and L. E. Larson, "Distortion in current commutating passive CMOS downconversion mixers," *IEEE Trans. Microw. Theory Techn.*, vol. 57, no. 11, pp. 2671–2681, Nov. 2009.

[11] W. Li, Y. Zhang, J. Wang, L.-K. Huang, J. Xiong, and C. Maple, "Diode-based IQ imbalance estimation in direct conversion transmitters," *Electron. Lett.*, vol. 50, no. 5, pp. 409–411, Feb. 2014.

[12] W. Li, Y. Zhang, L.-K. Huang, J. Cosmas, C. Maple, and J. Xiong, "Self-IQ-demodulation based compensation scheme of frequency-dependent IQ imbalance for wideband direct-conversion transmitters," *IEEE Trans. Broadcast.*, vol. 61, no. 4, pp. 666–673, Dec. 2015.

[13] M. A. I. Elmala and S. H. K. Embabi, "Calibration of phase and gain mismatches in weaver image-reject receiver," *IEEE J. Solid-State Circuits*, vol. 39, no. 2, pp. 283–289, Feb. 2004.